Calcified Tissue International

Cortical histomorphometry of the human humerus during ontogeny

--Manuscript Draft--

Manuscript Number:	CTIN-D-16-00424R3
Full Title:	Cortical histomorphometry of the human humerus during ontogeny
Article Type:	Original Article
Funding Information:	
Abstract:	Modeling and remodeling are two key determinants of human skeletal growth though little is known about the histomorphometry of cortical bone during ontogeny. In this study we examined the density and geometric properties of primary and secondary osteons (osteon area and diameter, vascular canal area and diameter) in sub-periosteal cortical bone from the human humerus (n=84) between birth and age 18 years. Sections were removed from the anterior midshaft aspect of humeri from skeletons. Age-at-death was reconstructed using standard osteological techniques. Analyses revealed significant correlation between the histomorphometric variables and age. Higher densities of primary osteons occurred between infancy and seven years of age but were almost completely replaced by secondary osteons after 14 years of age. The geometry of primary osteons was less clearly related to age. Secondary osteons were visible after two years of age, and reached their greatest densities in the oldest individuals. Osteon size was positively but weakly influenced by age. Our data implies that modeling and remodeling are age dependent processes that vary markedly from birth to adulthood in the human humerus.
Corresponding Author:	Rosie Pitfield, M.Sc University of Kent Canterbury, Kent UNITED KINGDOM
Corresponding Author Secondary Information:	
Corresponding Author's Institution:	University of Kent
Corresponding Author's Secondary Institution:	
First Author:	Rosie Pitfield, M.Sc
First Author Secondary Information:	
Order of Authors:	Rosie Pitfield, M.Sc
	Justyna J Miszkiewicz, PhD
	Patrick Mahoney, PhD
Order of Authors Secondary Information:	
Author Comments:	Dear Professor René Rizzoli Thank you for accepting my manuscript for publication in Calcified Tissue International. I have made the final corrections to the manuscript, which are highlighted in blue font in the revised version. Yours Sincerely Rosie Pitfield
Response to Reviewers:	Dear Professor René Rizzoli Thank you for accepting my manuscript for publication in Calcified Tissue International. I have made the final corrections to the manuscript, which are highlighted in blue font in the revised version. Yours Sincerely Rosie Pitfield

Cortical histomorphometry of the human humerus during ontogeny

Rosie Pitfield[a], Justyna J. Miszkiewicz[b], Patrick Mahoney[a]

[a]Human Osteology Lab, Skeletal Biology Research Centre, School of Anthropology and Conservation, University of Kent, Canterbury, United Kingdom.

[b]Skeletal Biology and Forensic Anthropology Research Group, School of Archaeology and Anthropology, The Australian National University, Canberra, Australia.

Correspondence: Rosie Pitfield

Human Osteology Lab, Skeletal Biology Research Centre,

School of Anthropology and Conservation,

University of Kent, Canterbury. UK. CT2 7NR.

E: rjp41@kent.ac.uk

T: +44 1227 82 3982

Abstract

Modeling and remodeling are two key determinants of human skeletal growth though little is known about the histomorphometry of cortical bone during ontogeny. In this study we examined the density and geometric properties of primary and secondary osteons (osteon area and diameter, vascular canal area and diameter) in sub-periosteal cortical bone from the human humerus (n=84) between birth and age 18 years. Sections were removed from the anterior midshaft aspect of humeri from skeletons. Age-at-death was reconstructed using standard osteological techniques. Analyses revealed significant correlation between the histomorphometric variables and age. Higher densities of primary osteons occurred between infancy and seven years of age but were almost completely replaced by secondary osteons after 14 years of age. The geometry of primary osteons was less clearly related to age. Secondary osteons were visible after two years of age, and reached their greatest densities in the oldest individuals. Osteon size was positively but weakly influenced by age. Our data implies that modeling and remodeling are age dependent processes that vary markedly from birth to adulthood in the human humerus.

Key Words

Primary osteon; secondary osteon; modeling; remodeling; humerus, cortex

Introduction

Current understanding of human cortical bone histomorphometry during ontogeny is limited. Histomorphometric studies have explored cortical drift, the gross geometry of the human femur [1, 2] and humerus [3-5], and bone remodeling with age in the iliac bone [6]. Recently, relationships between secondary osteon area and mechanical loading have been reported for the femur, humerus and rib [7]. Following earlier observations that osteon frequency increases with age [8], qualitative analyses of rib bone histology have been incorporated into methods for reconstructing juvenile age-at-death [9]. Collectively, these studies have begun to characterize ontogenetic change in human bone microstructure, and how this variation relates to macroscopic indicators of bone growth.

Describing age-related changes in cortical bone tissue may be useful to better understand juvenile fracture risk. Fracture risk is partially dependent on bone strength, which in turn is dependent on bone composition [10, 11]. Primary bone has different mechanical properties compared to secondary bone, which is related in part to differences in microstructure. For example, the presence of primary or secondary osteons can affect bone density, and modulus of elasticity just prior to failure, which has been linked to different types of childhood fractures [10, 11]. Unfortunately, studies describing age-related variation in the histomorphometry of primary and secondary osteons in human cortical bone are still limited [6, 12]. Thus we decided to explore the density and geometric properties of osteons in human humeral cortical bone during ontogeny. For that purpose we used a skeletal collection available in Canterbury, UK. Our data can provide a new insight into one factor that contributes to juvenile fracture risk.

Growth of the human humerus

The human humerus attains its adult shape and size through an ontogenetic growth phase that encompasses two physiological processes - modeling and remodeling [12]. Modeling largely involves the deposition of primary bone tissue onto a cartilaginous model of bone. Primary osteons can form when existing blood vessels become entrapped in the bone matrix at the bone surfaces during appositional growth [3, 13] and during lamellar compaction [4], when trabecular spaces are 'in-filled' to from cortical bone [12]. Unlike modeling, remodeling primarily replaces existing bone with new bone through the linked action of osteoclasts and osteoblasts (Bone Multicellular Units - BMUs) to produce secondary osteons [14]. Together, these processes lead to the attainment of a mostly genetically determined adult bone size and morphology [3], though mechanical load, diet, and hormones, amongst other factors, influence humeral growth during ontogeny [7]. The spatial distribution of bone tissues changes through ontogeny with an overall trend for immature woven bone to be replaced first by primary lamellar bone, and then secondary bone in the form of secondary osteons that are surrounded by cement lines. Thus we expect primary osteon density to be negatively correlated with age, whilst secondary osteon population density should be positively correlated with age.

Previous studies investigating bone modeling in relation to the micro-strucutre of primary osteons have been based on experiments in non-human vertebrates such as birds [15], guinea pigs and monitor lizards [16], and sheep [17]. It has been shown that centripetal osteogenesis occurs during primary osteon formation in modeling in bird taxa [18], decreasing the size of vascular osteonal canals due to new lamellar bone apposition. It is currently unknown whether the few concentric lamellae that can be observed in primary osteons in human juveniles are formed by centripetal osteogenesis. If this process does occur in humans we would expect to see a reduction in primary vascular canal size with increasing age.

Bone morphology is partially influenced by mechanical loading. Modeling strengthens bone by increasing cross-sectional area, reducing compressive stress, and by sub-periosteal apposition to increase resistance to bending and twisting [19]. As a result, children who undertake intensive physical activity often develop more robust bones than those who are more sedentary [14]. Over time, stress may cause microscopic cracks (micro-damage) to appear and accumulate in the bone. Targeted remodeling (an estimated 30% of remodeling activity [20]) replaces these micro-cracks to maintain mechanical strength [14]. The cement lines of the secondary osteons prevent the spread of micro-cracks. In previous studies of adult bone smaller osteons are correlated with larger strains [21] and advancing age [22]. It is not known when this trend begins and it is possible that secondary osteon size will decrease throughout the juvenile period. Stochastic remodeling is not site dependent and is associated with mineral homeostasis [20]. Both targeted and stochastic remodeling are active through the entire human lifespan and so secondary osteons accrue with age [23].

Histomorphometric measurements of bone growth

Here, we calculate histomorphometric parameters of cortical bone growth for the human humerus, and assess these against age. Osteon population density is a measure of complete and fragmentary secondary osteons per section area, which together represent past remodeling events [24]. Primary osteon density, a feature of bone modeling, particularly in periosteal region of long bones [5, 13], can increase with age [e.g. 25]. The size and shape of primary canals can be an indicator of primary bone deposition during modeling [e.g. 16]. The size and shape of secondary osteons and their vascular canals has also been linked to age [e.g. 24], as well as mechanical stress [e.g. 22], diet [e.g. 26], and health [e.g. 27]. Based upon prior research we predict primary osteon density will decrease with age [5], while secondary osteon population

density will increase [3]. Primary osteon canal size will decrease with age [18], while secondary osteons will become smaller and more circular [22].

Samples and methods

Sample

The study sample comprised eighty-four human juvenile skeletons that did not retain skeletal evidence from pathology, or a healed fracture. Many of these skeletons have accompanying radiographs. Radiographs were produced at Kent and Canterbury Hospital (Radiology Department) for any skeleton with suspected trauma or skeletal pathology. The skeletons had previously been recovered from one cemetery in Canterbury, England, which dated to the 16th century. Historical texts state that the burials were from a single socio-economic group that lived and worked in Canterbury [28]. The skeletons are curated in the Skeletal Biology Research Centre, University of Kent, UK. No permits were required for the present study as these skeletal samples pre-date the Human Tissue Act. All sampling followed appropriate codes of ethics for research conducted on human skeletons [29]. These skeletons have previously been incorporated into a study that examined histomorphometric variables in adult femoral cortical bone [30].

Age

We used multiple standard osteological methods to reconstruct age-at-death for each skeleton, as the actual biological age of each skeleton was not known. Age-at-death estimations for juvenile skeletons are more accurate than those for adults. We collated several age-at-death estimates using established methods that rely upon the assessment of tooth formation times [31], timing of dental eruption [32], and fusion of cervical vertebrae [33]. Histomorphometric descriptive statistics were subdivided into four age groups, which were: Infant (0-1.9 years,

n=6), Young Child (2-7.9 years, n=42), Older Child, (8-12.9 years, n=22) and Adolescent (13-18 years, n=14). These age groups roughly correspond to different developmental phases of childhood growth, i.e. the accelerated growth rate in early childhood and adolescence. We were unable to account for any hormonal changes associated with puberty that may affect bone growth during adolescence in this sample as biological sex estimation based upon gross anatomical measurements from sub-adult skeletal remains is not possible.

Sample selection and preparation

One humerus was sampled from each skeleton. The right humerus (n=57) was selected based on availability of the midshaft for sectioning, meaning that the left humerus (n=27) was only chosen as a substitute when the right side was not preserved. The humerus was selected because the cortical area is large enough to study histologically in perinatal remains. Furthermore, the histomorphometry of the human humerus is less well described in the literature, relative to the femora and ribs [1, 7, 9, 25].

Standard histological methods were used [e.g. 34, 35]. Thin sections were removed from the anterior midshaft region (located by dividing the maximum length - or diaphyseal length where epiphyses were not united with the shaft - of the complete humerus by two). When the humerus was fragmented, the midshaft was located by comparing it to the complete antimere. Removing anterior sections is less destructive than removing entire cross sections and preserves the bone for future study. All sections were removed using an electronic drill (Dremel Rotary Tool®). Each section removed was approximately 0.7±0.2cm thick. Sections were embedded in resin (Buehler EpoxiCure®), further reduced to 0.3±0.1cm using a Buehler Isomet 4000 precision saw, and fixed to glass microscope slides (Evo Stick® resin). Each section was ground (Buehler EcoMet 300), polished with a 0.3µm aluminum oxide powder (Buehler® Micro-

Polish II), cleaned in an ultrasonic bath, dehydrated in 95-100% ethanol, cleared (Histoclear®), and mounted with a coverslip using a xylene-based medium (DPX®).

Microscopy

Imaging and histomorphometric procedures followed standard methods [e.g. 30, 35]. Imaging was undertaken using an Olympus BX51 compound microscope with an Olympus DP25 microscope camera. Figure 1a illustrates that images were obtained from five regions of interest (**ROIs**) using CELL® Live Biology Imaging software. Each section was divided into locations: medial (**1**), antero-medial (**2**), anterior (**3**), antero-lateral (**4**), and lateral (**5**).

Each ROI within each of these locations was positioned sub-periostealy in the cortex to exclude the endosteal and periosteal surfaces that have non-remodeled interstitial lamellae in juveniles [1]. In addition, given the increased bone resorption in the endosteum and increased bone formation in the periosteum during modeling, bone sites in the subperiosteal region should reflect osteons that can be, at least partly, associated with age related growth of the cortex. Because our study examines samples from a series of bones representing individuals of different ages, we acknowledge that the overall size of bone differs inter-individually. However, selecting ROIs in a relatively consistent way allows us to undertake comparisons between data sampled from the same region of the bone. Sometimes the ROI would have to be moved fractionally to avoid diagenesis and taphonomy. However, the ROI would still be within the medial, anteromedial, medial, anterolateral, or lateral compartment of the section (ie., medial would still be medial).

The number of primary osteons, secondary osteons, and secondary osteon fragments were counted in each ROI at a magnification of 10x. Primary osteons (**Fig. 1b**) were identified by a Haversian circular canal that is surrounded by few, if any, circumferential lamellae. Secondary osteons (**Fig. 1c**) were identified by cement lines [13], and fragments were identified as partial

secondary osteons with more than 10 percent of the Haversian canal remodeled by subsequent secondary osteons [25]. The osteon counts formed two density variables, which were calculated by dividing the number of osteons by the area of the ROI (2.24mm^2):

1. Primary Osteon Density: Pr.On = #Pr.On./2.24. In the absence of a cement line, we used the presence of one Haversian primary canal as a proxy for one primary osteon.
2. Osteon population density: OPD = (N.On.+N.On.Fg.)/2.24. Only osteons that had identifiable cement lines that were over 90% intact were counted as complete secondary osteons. Osteon fragments were identified as partial osteons with more than 10% of the Haversian canal showing evidence of remodeling [25].

Each ROI was subdivided into quarters resulting in four sub-ROIs for the purpose of increasing measurement accuracy. Osteonal geometric properties (**Fig. 1d**) were measured in each subdivision at a magnification of 20x. At this level of magnification the following features were measured in µm^2:

3. Primary Osteons: canal area (Pr.On.Ar), minimum diameter (Pr.On.Dm$_{min}$), maximum diameter (Pr.On.Dm$_{max}$)

4. Secondary Intact Osteons: area (On.Ar), minimum diameter (On.Dm$_{min}$), maximum diameter (On.Dm$_{max}$). Haversian canal area (H.Ar), minimum canal diameter (H.Dm$_{min}$), maximum canal diameter (H.Dm$_{max}$). The average value was calculated for each variable, from all ROI's combined, for each individual.

Statistical Analyses

Data were analyzed in IBM SPSS® 22 (2014). A one-sample Kolmogorov-Smirnov test indicated that distribution of the data for each variable was normal. Data from right and left humeri were pooled into a single sample. The strength of the relationship between the age of each individual, and each histomorphometric variable, was assessed using correlation and linear

regression statistics. In linear regressions, r values indicate the proportion of variance in the dependant variable that is explained by the independent variable. A residual value is the error not explained by the regression equation. Further comparisons between histomorphometric variables when sub-divided by age groups were undertaken using a non-parametric Kruskal-Wallis test combined with a Dunn-Bonferroni post hoc test.

Results

Osteon density and age

Descriptive statistics subdivided by age group are in Table 1. Comparisons between the age groups are in Table 2 and Table 3. Some individuals did not have both primary and secondary osteons visible within the ROIs resulting in different sample sizes in Table 2. The density of primary osteons differed significantly between age groups. Post-hoc tests revealed that adolescents had a significantly reduced density of primary osteons compared to all younger childhood age-groups. Older children also had a reduced Pr.On compared to infants. Regression statistics are in Table 4. The density of primary osteons was significantly and negatively correlated with age, decreasing from infants to adolescents (**Fig. 2a**). Primary osteons were almost absent after age 14 years.

Secondary osteon population density differed significantly between the groups. Adolescents had a significantly greater secondary osteon population density compared to younger childhood age-groups. Older children also had a greater OPD compared to the younger childhood age group and infants. In contrast to primary osteon density, the number of secondary osteons was significantly and positively correlated with age (**Fig. 2b**). Secondary osteons were absent until after two years of age, and the greatest density occurred amongst adolescents.

Osteon size and age

Comparisons between the age groups revealed that the minimum diameter of primary osteon vascular canals amongst the adolescents was significantly larger, and the maximum diameter was significantly smaller, compared to all of the younger age groups. Regression analyses revealed that primary osteon vascular canal area did not correspond with the age of the juveniles (**Fig. 3a**).

Secondary osteons of adolescents had a significantly greater area, and their maximum diameter was significantly larger, relative to the younger childhood age group. Haversian canals of adolescents also had a significantly smaller minimum diameter, and larger maximum diameter, compared to the other younger childhood age groups.Secondary osteon area increased significantly with age (**Fig. 3b**), which was associated with an increase in maximum diameters. Regression analyses revealed that the area of secondary osteons was also significantly and positively correlated with the density of secondary osteons ($r=0.63$; $p=0.00$). The minimum and maximum diameters of secondary osteon Haversian canal area increased with age, though the residual associated with these correlations was high.

Discussion

Here, we examined the density and geometric properties of both primary and secondary osteons in cortical bone from the anterior mid-shaft region of the human humerus. We have expanded upon recent research into the histology of the humerus [3, 5, 7], by assessing parameters of cortical bone modeling and remodeling between birth and 18 years of age. Our study shows that the density of both osteon types is linked to age, but the relationship between age and osteon geometry is more complicated.

Age related change in primary osteons

As primary osteons form around vascular canals by becoming entrapped by lamellar bone tissue during growth, our data suggest that modeling at the periosteal envelope producing primary osteons may peak by seven years of age. In our sample, there were hardly any primary osteons remaining in the sub-periosteal region of the humeri of the eldest children. Neither did the size of the primary vascular canals change greatly with age. At present, our understanding of primary osteon formation in humans is still limited, but based on previous experimental research on animals it is thought that primary vascular canals are 'in-filled' by bone deposition [16]. Therefore, it might be expected that primary osteon canal area would decrease with advancing age if they form in the same way in human cortical bone. Our data do not support this idea, though there are several reasons why the association between canal area and age may not be present in our sample. Relatively decreased canal size might become apparent when compared within one age group, rather than when compared between children of different age. Prior research on adult cortical bone also reports inconsistent association with age [22, 36].

Age related change in secondary osteons

Primary osteons are gradually replaced by secondary osteons through remodeling [34], resulting in an increase in the number and density of secondary osteons as bone ages. The correlation between an increasing density of secondary osteons and advancing age is well documented in adult bone [8, 24], and has previously been confirmed in the juvenile humerus [4]. However, our data reveal that secondary osteons were present in early childhood from two years of age, and after 14 years of age the subperiosteal region of the anterior mid-shaft humerus is composed of mainly secondary osteonal bone. This finding is similar to results reported for the femur [25], where secondary osteons were also present in children between the age of 6 to 10 years. Cambra-Moo and colleagues [3] report that Haversian bone accounted for 47.37%

and 78.67% respectively of the entire cortical area of the humeri of two juveniles aged between 10 and 20 years.

Approximately three quarters of childhood fractures occur in the upper limbs [37]. Fracture risk varies with age but seems to peak during early adolescence [37]. The change from primary and secondary bone, to predominantly secondary osteonal bone at around 14 years of age in our data (Fig 4a-b), could be one factor that contributes to the increased fracture risk of adolescents relative to younger children. For example, cement lines of secondary osteons have been shown to be sites of weakness [38] and remodeled bone is more brittle than primary lamellar bone [11]. The presence of mainly secondary osteonal bone from 14 years of age also coincides with peak bone mineral accrual rates (females=13yrs, males=14ys) reported in a study of Canadian children and young adults [39].

Our results for the geometric properties of secondary osteons in the humerus are similar to those reported for the ilium [6]. Generally, the size of secondary osteons and their vascular canals did not change greatly with age, relative to the relationship between the density of secondary osteons and age. When the size of osteons changed, there was substantial variation between individuals, which has been reported previously [36]. However, some trends can still be discerned. Secondary osteons become larger with age (r=0.40) with a clear increase in their maximum diameter (r=0.52). When compared between the age groups, mean secondary osteon area of 40239.09μm^2 and maximum diameter of 364.09μm for adolescents was significantly greater compared to the younger childhood age group (area=30844.68μm^2, max diameter=265.91μm). These values are within the range of mean osteon areas (20184μm^2 to 64391μm^2) reported for iliac cortices of juveniles, aged between birth and 25 years, [40]. However, in a sample of juvenile transiliac sections there was no significant correlation between osteon diameter and age [6]. This difference between studies may represent underlying age-related differences in remodeling activity between the humerus and ilium, or population

differences. Intra-skeletal variation in osteonal bone has been recently observed in a juvenile skeletal sample [7]. Alternatively, it might reflect the different measurements employed in the two studies. Rauch and colleagues [6] measured one diameter dimension, but our data showed a correlation between age and maximum diameter.

We observed a significant trend in the dimensions of secondary Haversian canals, when compared between age groups. Vascular canals of secondary osteons become more irregular with increasing age. This is because canal minimum diameters became smaller, ranging from 26.82µm in young children to 19.19µm in adolescents, while maximum diameter becomes larger, ranging from 72.63µm in young children to 99.47µm in adolescents. There was no associated change in canal area with age. Contrary to the results presented here, Rauch and colleagues [6] found no significant correlation between secondary vascular canal diameter and age. Although, as with secondary osteon diameters, only one measure of diameter was taken rather than maximum and minimum dimensions.

Secondary osteon size is determined by the amount of bone that is removed by osteoclasts [25]. In principle, the wider the resorption diameter the larger the resulting osteon will be. Osteoblasts subsequently deposit bone within the osteon from the cement line inwards towards the center, determining the size of the Haversian canal [41]. Thus, the area and diameter of osteon and Haversian canal transverse surfaces viewed in thin sections should be an indicator of BMU activity. Larger osteons of older children may indicate a slower rate of BMU activity because it takes longer to remove a large area of bone and deposit more lamellae [42], or, it may reflect an increase in osteoclast resorption resulting in ‘tunneling’ larger osteons composed of larger vascular canals. These age-related changes in the morphology of secondary osteons in juveniles exhibit a different pattern compared to those of adults.

As discussed previously, in adult bone, the change in the size of secondary osteons in relation to age is still not fully understood [22], especially as variation in osteon geometric

properties may relate to the type of load that bone is exposed to. Smaller and more circular osteons have been linked to compressive forces, and larger and less circular osteons have been shown to correspond to tensile forces [43]. If these findings are applied to our data, then perhaps bone remodeling in the subperiosteal region of the anterior humerus was influenced by tensile load during adolescence in response to upper arm physical activity. We were unable to investigate the effect of mechanical loading on bone histology in our skeletal sample, which could have contributed to the variation in secondary osteonal structure with age.

Alternatively, the apparent increase in maximum diameter of secondary osteons may be the result of an accumulation of mature drifting osteons. Drifting osteons are a type of secondary osteon with continuous resorption and continuous formation at opposite sides of the osteon, resulting in a transverse elongation in the horizontal plane [44]. Early histological studies found that drifting osteons occur most commonly in sub-adult bone [45]. Indeed, drifting osteons have been observed in the juvenile humerus [4], rib [9], and femur [1]. However, the biomechanical implications of drifting osteons in juvenile cortex remain poorly understood [44].

When the structure and density of secondary osteons are considered together, it suggests that adolescents have a greater number of these bone functional units, which are slightly larger with more irregular vascular canals, relative to younger children and infants. Although some characteristics of primary and secondary osteons are age-related, other factors will also exert an influence. Differences in secondary osteon structure and density between studies imply that there is substantial variation between human populations, and so in order to expand our understanding of human humeral bone growth further research is needed to gain more representative sampling from different human populations to establish the range of bone microstructural variability.

There are several limitations within our study. The sample was undocumented so age-at-death was estimated using multiple standard osteological methods. Even though age-at-death estimations for juvenile skeletons are more accurate than those for adults, these estimates may have introduced variation into our analyses of histomorphometry and age. The uneven sample sizes in each age group in this study reflect the pattern of infant mortality in medieval Canterbury. Additionally it is possible that aspects of cortical bone growth have changed since the medieval period. Future studies on known age and sex populations can expand upon our study.

Conclusion

This study has shown that the density of primary and secondary osteons is markedly age related in the human humerus, but the relationship between the geometric properties of bone modeling and remodeling units and age is more complicated. Future studies might further explore how other factors affect the age-related change in juvenile bone microstructure by examining sex, puberty, biomechanics, or diet to reveal broader perspectives into skeletal growth.

References

[1] Goldman HM, McFarlin SC, Cooper DML, et al (2009) Ontogenetic patterning of cortical bone microstructure and geometry at the human mid-shaft femur. Anat Rec 292:48–64. doi: 10.1002/ar.20778

[2] Maggiano IS, Maggiano CM, Tiesler VG, et al (2015) Drifting diaphyses: Asymmetry in diametric growth and adaptionalong the humeral and femorallength. Anat Rec 298:1689–1699. doi: 10.1002/ar.23201

[3] Cambra-Moo O, Nacarino Meneses C, Rodríguez Barbero MÁ, et al (2014) An approach to the histomorphological and histochemical variations of the humerus cortical bone through human ontogeny. J Anat 224:634–646. doi: 10.1111/joa.12172

[4] Maggiano CM (2012) Histomorphometry of humeral primary bone: evaluating the endosteal lamellar pocket as an indicator of modeling drift in archaeological and modern skeletal samples. PhD Dissertation.

[5] Maggiano CM, Maggiano IS, Tiesler VG, et al (2016) Methods and theory in bone modeling drift: Comparing spatial analyses of primary bone distributions in the human humerus. J Anat 228:190–202. doi: 10.1111/joa.12383

[6] Rauch F, Travers R, Glorieux FH (2007) Intracortical remodeling during human bone development-A histomorphometric study. Bone 40:274–280. doi: 10.1016/j.bone.2006.09.012

[7] Eleazer CD, Jankauskas R (2016) Mechanical and metabolic interactions in cortical bone development. Am J Phys Anthropol 160:317–333. doi: 10.1002/ajpa.22967

[8] Kerley ER (1965) The microscopic determination of age in human bone. Am J Phys Anthr 23:149–163

[9] Streeter M (2010) A four-stage method of age at death estimation for use in the subadult rib cortex. J Forensic Sci 55:1019–1024. doi: 10.1111/j.1556-4029.2010.01396.x

[10] Martin RB, Burr DB, Sharkey NA, Fyhrie DP (2015) Skeletal tissue mechanics. Springer

[11] Ogden JA (2006) Skeletal injury in the child. Springer Science & Business Media

[12] Maggiano CM (2011) Making the mold: A microstructural perspective on bone Modeling during growth and mechanical adaption. In: Crowder C, Stout SD (eds) Bone histology: An anthropological perspective. CRC Press, pp. 45–90

[13] Currey JD (2002) Bones: structure and mechanics. Princeton University Press

[14] Robling AG, Castillo AB, Turner CH (2006) Biomechanical and Molecular Regulation of Bone Remodeling. AnnuRev Biomed Eng 8:455–98. doi: 10.1146/annurev.bioeng.8.061505.095721

[15] De Margerie E, Robin J-P, Verrier D, et al (2004) Assessing a relationship between bone microstructure and growth rate: a fluorescent labelling study in the king penguin chick (Aptenodytes patagonicus). J Exp Biol 207:869–879. doi: 10.1242/jeb.00841

[16] Cubo J, Legendre P, De Ricqlès A, et al (2008) Phylogenetic, functional, and structural components of variation in bone growth rate of amniotes. Evol Dev 10:217–227. doi: 10.1111/j.1525-142X.2008.00229.x

[17] Cambra-Moo O, Nacarino-Meneses C, Díaz-Güemes I, et al (2015) Multidisciplinary characterization of the long-bone cortex growth patterns through sheep's ontogeny. J Struct Biol 191:1–9. doi: 10.1016/j.jsb.2015.06.013

[18] Starck JM, Chinsamy A (2002) Bone microstructure and developmental plasticity in birds and other dinosaurs. J Morphol 254:232–246. doi: 10.1002/jmor.10029

[19] Lieberman DE, Devlin MJ, Pearson OM (2001) Articular area responses to mechanical loading: Effects of exercise, age, and skeletal location. Am J Phys Anthropol 116:266–277. doi: 10.1002/ajpa.1123

[20] Burr DB (2002) Targeted and nontargeted remodeling. Bone 30:2–4. doi: 10.1016/S8756-3282(01)00619-6

[21] van Oers RF, Ruimerman R, Tanck E, et al (2008). A unified theory for osteonal and hemi-osteonal remodelling.Bone 42(2):250-259

[22] Britz HM, Thomas CDL, Clement JG, Cooper DML (2009) The relation of femoral osteon geometry to age, sex, height and weight. Bone 45:77–83. doi: 10.1016/j.bone.2009.03.654

[23] Stout S, Crowder C (2011) Bone remodeling, histomorphology, and histomorphometry. In: C. Crowder, S. Stout (eds) Bone histology: An anthropological perspective. CRC Press, pp. 23–44

[24] Frost HM (1987) Secondary osteon populations: An algorithm for determining mean bone tissue age. Am J Phys Anthropol 30:221–238. doi: 10.1002/ajpa.1330300512

[25] Caccia G, Magli F, Tagi VM, et al (2016) Histological determination of the human origin from dry bone: a cautionary note for subadults. Int J Legal Med 130:299–307. doi: 10.1007/

[26] Paine RR, Brenton BP (2006) Dietary health does affect histological age assessment: An evaluation of the Stout and Paine (1992) age estimation equation using secondary osteons from the rib. J Forensic Sci 51:489–492. doi: 10.1111/j.1556-4029.2006.00118.x

[27] Storm T, Steiniche T, Thamsborg G, Melsen F (1993) Changes in bone histomorphometry after long-term treatment with intermittent, cyclic etidronate for postmenopausal osteoporosis. J Bone MinerRes 8:199–208. doi: 10.1002/jbmr.5650080211

[28] Duncombe J, Batterly N (1785) The history and antiquities of the three archiepiscopal hospitals and other charitable foundations at and near Canterbury. Bibliotheca Topographica Britannica No XXX. London

[29] Mays S, Elders J, Humphrey L, White W, Marshall P (2013) Science and the Dead: A guidelines for the destructive sampling of archaeological human remains for scientific analysis. Advisory Panel on the Archaeology of Burials in England. English Heritage

[30] Miszkiewicz JJ, Mahoney P (2016) Ancient human bone microstructure in Medieval England: Comparisons between two socio-economic groups. Anat Rec 299:42–59. doi: 10.1002/ar.23285

[31] Moorrees CF, Fanning E a, Hunt EE (1963) Age variation of formation stages for ten permanent teeth. J Dent Res 42:1490–1502. doi: 10.1177/00220345630420062701

[32] Al Qahtani SJ, Hector MP, Liversidge HM (2010) Brief communication: The London atlas of human tooth development and eruption. Am J Phys Anthropol 142:481–490. doi: 10.1002/ajpa.21258

[33] Scheuer L, Black S (2000) Development and ageing of the juvenile skeleton. In: Cox M, Mays S (eds) Hum Osteol Archaeol Forensic Sci. London: Greenwich Medical Media Ltd pp 9–21

[34] Crowder C, Stout S (2011) Bone Histology: An Anthropological Perspective. CRC Press

[35] Villa C, Lynnerup N (2010) Technical note: A stereological analysis of the cross-sectional variability of the femoral osteon population. Am J Phys Anthropol 142:491–496. doi: 10.1002/ajpa.21269

[36] Pfeiffer S (1998) Variability in osteon size in recent human populations. Am J Phys Anthropol 106:219–227. doi: 10.1002/(SICI)1096-8644(199806)106:2<219::AID-AJPA8>3.0.CO;2-K

[37] Goulding A(2007) Risk factors for fractures in normally active children and adolescents. In:Daly R, Petit M (eds) Optimizing bone mass and strength; the role of physical activity and nutrition during growth. Med Sport Sci. Karger, Basel, vol 51, pp 102-120 (DOI:10.1159/000103007)

[38] Carter DR, Spengler DM (1978) Mechanical properties and composition of cortical bone. Clin OrthopRelat R 135:192-217

[39] Baxter-Jones AD, Faulkner RA, Forwood MR, et al (2011). Bone mineral accrual from 8 to 30 years of age: an estimation of peak bone mass. J Bone Miner Res 26(8):1729-1739

[40] Schnitzler CM, Mesquita JM (2013) Cortical porosity in children is determined by age-dependent osteonal morphology. Bone 55:476–486. doi: 10.1016/j.bone.2013.03.021

[41] Skedros JG, Knight AN, Clark, GC, et al(2013) Scaling of Haversian canal surface area to secondary osteon bone volume in ribs and limb bones. Am J Phys Anthropol 151(2):230-244

[42] Pfeiffer S, Crowder C, Harrington L, Brown M (2006) Secondary osteon and Haversian canal dimensions as behavioral indicators. Am J Phys Anthropol 131:460–468. doi: 10.1002/ajpa.20454

[43] Skedros JG, Mason MW, Bloebaum RD (1994) Differences in osteonal micromorphology between tensile and compressive cortices of a bending skeletal system: Indications of potential strain- specific differences in bone microstructure. Anat Rec 239:405–413. doi: 10.1002/ar.1092390407

[44] Robling AG, Stout SD (1999) Morphology of the drifting osteon. Cells Tissues Organs 164:192–204. doi: 10.1159/000016659

[45] Sedlin ED, Frost HM, Villanueva AR (1963) Variations in cross-section area of rib cortex with age. J Gerontol 18:9–13.

Fig. 1 (a) Anterior mid-shaft humerus region with five regions of interest (1-5), used for counting primary and secondary osteons (10x), and measuring osteonal structure (20x)**.** Primary osteon **(b)** and secondary osteon **(c)** micrographs (20x magnification). White arrows point to vascular canals. **(d)** Micrograph (20x magnification) illustrating the different histology variables examined in the present study. Areas highlighted in orange indicate an intact (top) and a fragmentary (bottom) secondary osteon (N·On, N·On·Fg, and OPD). White circles indicate the secondary osteon and canal areas measured (On·Ar, and H·Ar). Dashed lines indicate minimum and maximum diameters of secondary osteon (top) and canal (bottom) (On·Dm_{max}, On·Dm_{min}, H·Dm_{max}, H·Dm_{min}). White arrows indicate osteocyte lacunae (Ot·Dn)

Fig. 2 (a) Plot of primary osteon density, and **(b)** secondary osteon population density, against the age of the children. Linear regression lines are fitted to the data. Regression equations for cortical bone are in Table 1

Fig. 3 (a) Plot of primary osteon canal area, and **(b)** secondary osteon area, against the age of the children. Linear regression lines are fitted to the data. Regression equations for cortical bone are in Table 1

Figure

Click here to download Figure Fig 1.tif

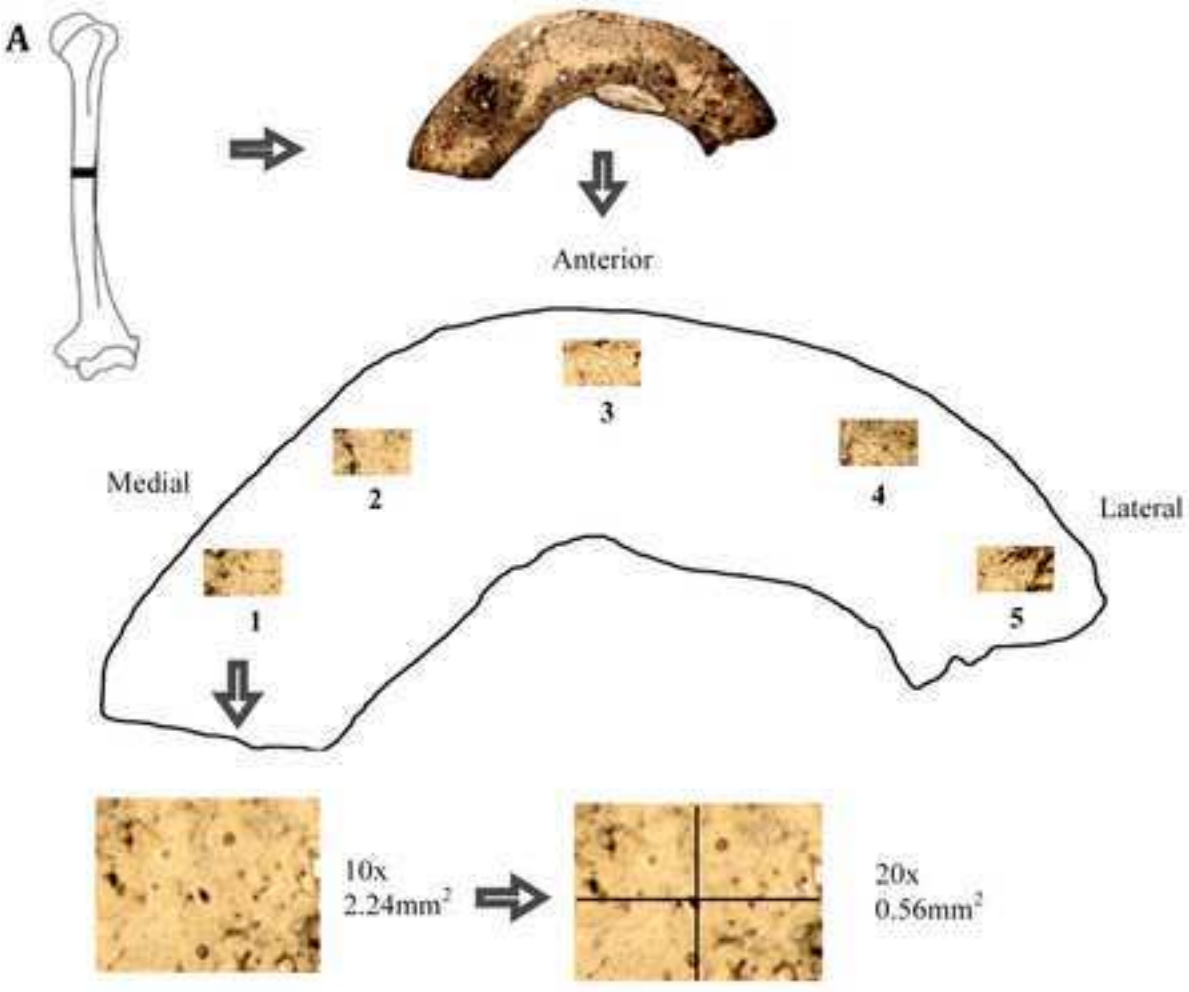

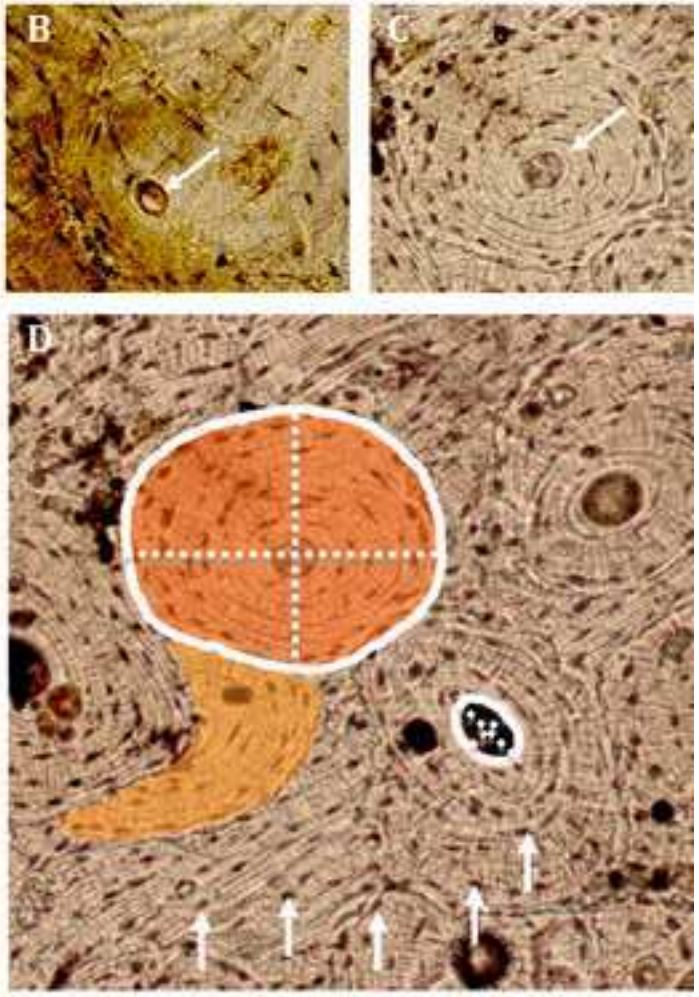

Figure

Click here to download Figure Fig 2.tif

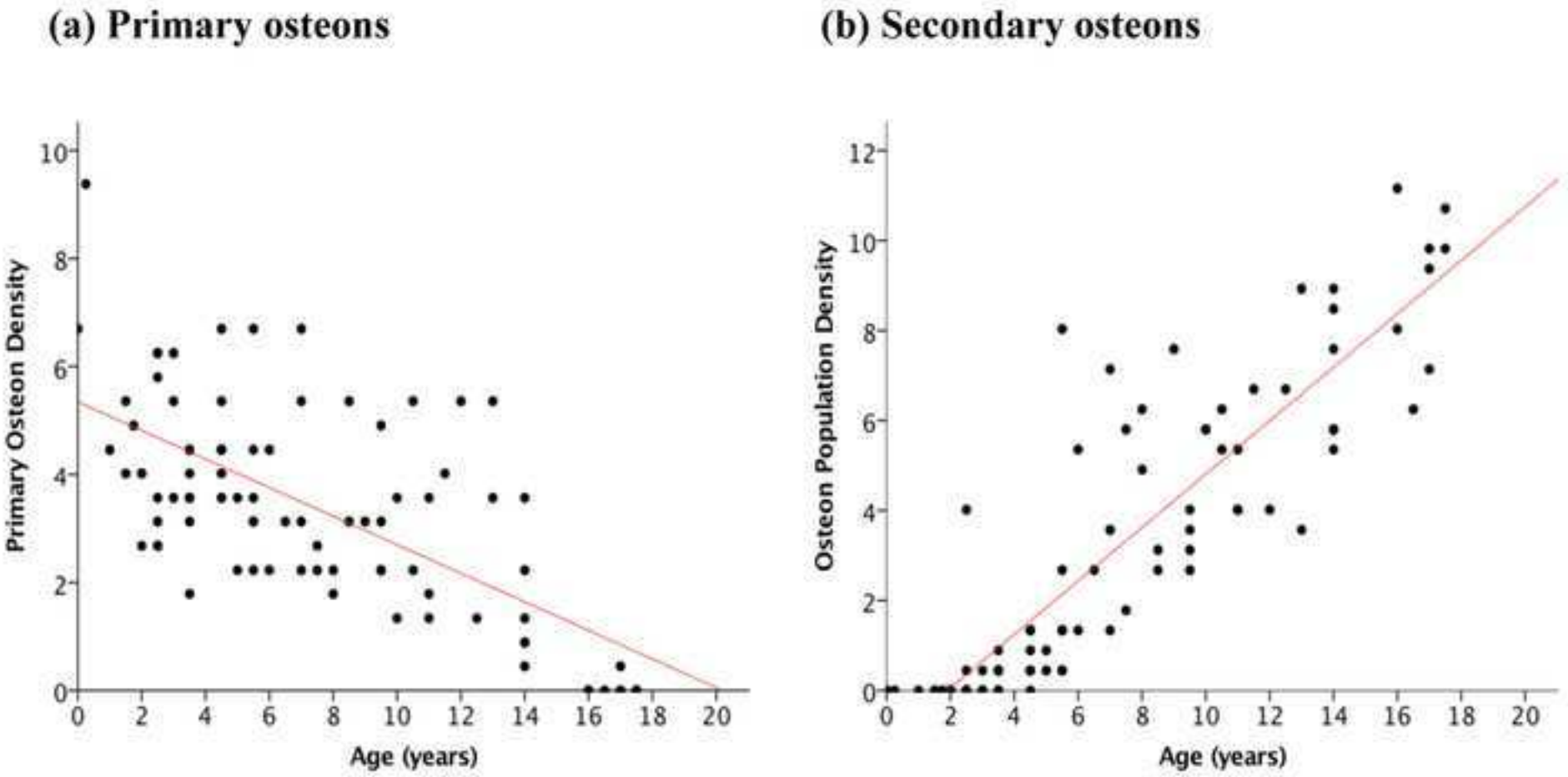

Figure

Click here to download Figure Fig 3.tif

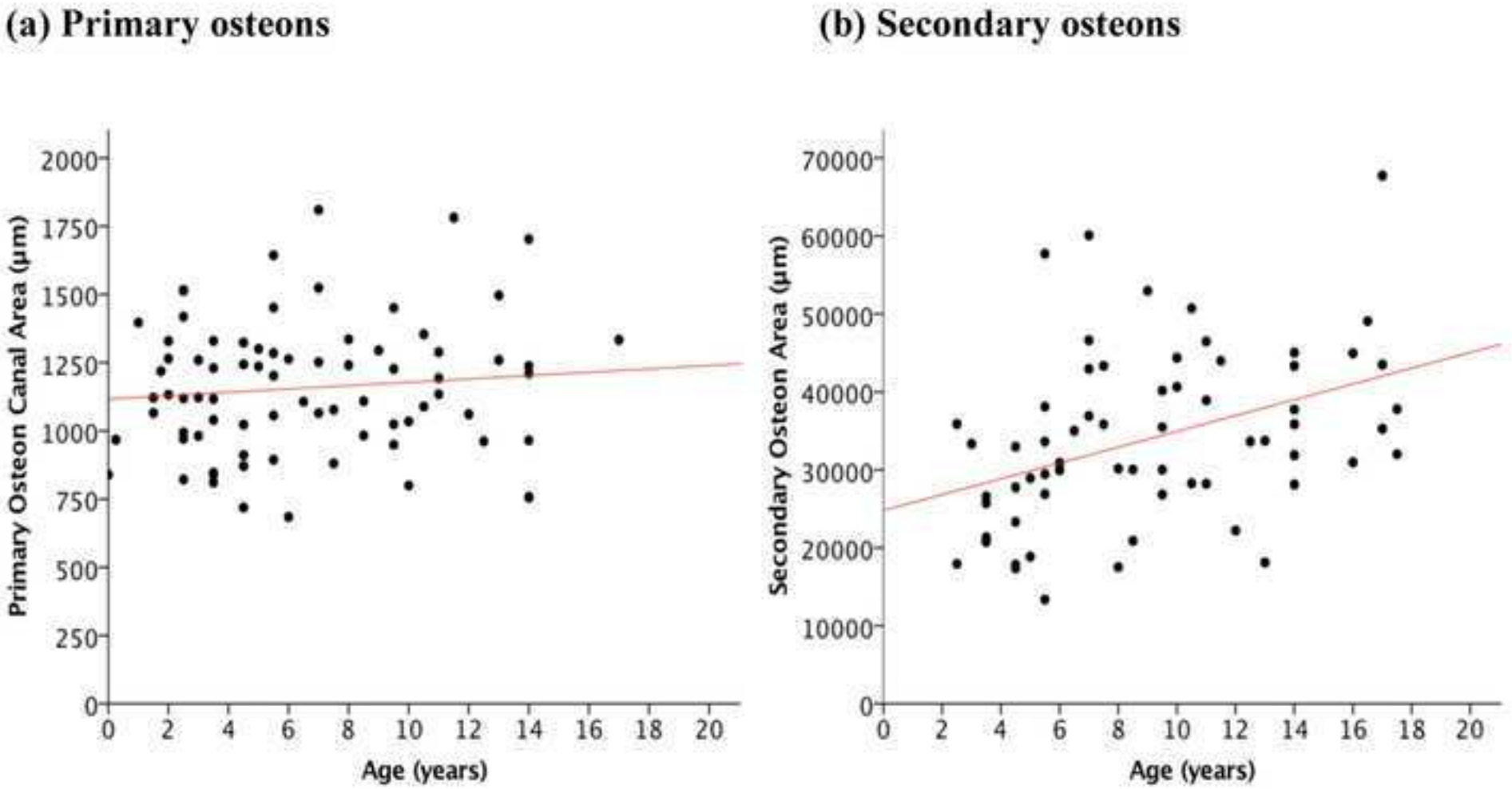

Table 1 Histomorphometric descriptive statistics subdivided into age groups

		Infant	Young child	Older child	Adolescent
		birth to 1.9	2 to 7.9	8 to 12.9	13 to 18
Histomorphometric variable		n= 6	n= 42	n= 22	n= 14
Number of Primary Osteons	Mean	13.00	9.00	7.05	1.57
	SD	4.43	3.08	3.15	2.38
Number of Secondary Osteons	Mean	0.00	2.76	9.36	14.79
	SD	0.00	3.72	3.40	3.66
Number of Secondary Osteon Fragments	Mean	0.00	0.36	1.45	3.50
	SD	0.00	0.98	1.10	1.91
Primary Osteon Density	Mean	5.47	4.01	3.14	0.70
	SD	1.31	1.37	1.40	1.06
Secondary Osteon Population Density	Mean	0.00	1.39	4.82	8.16
	SD	0.00	2.02	1.79	1.91
Primary Canal Area	Mean	1101.75	1157.88	1179.45	1137.66
	SD	194.89	252.97	226.38	339.37
Primary Canal Minimum Diameter	Mean	17.86	18.90	18.78	23.540
	SD	4.08	2.97	4.07	4.83
Primary Canal Maximum Diameter	Mean	69.72	67.61	66.04	49.06
	SD	14.10	14.66	13.25	6.42
Secondary Osteon Area	Mean		30844.68	34059.09	40239.09
	SD		11450.67	10029.61	10102.21
Secondary Osteon Minimum Diameter	Mean		129.78	124.00	121.84
	SD		23.96	27.81	18.07
Secondary Osteon Maximum Diameter	Mean		265.91	317.63	364.09
	SD		80.67	72.70	59.58
Secondary Canal Area	Mean		1876.84	1827.63	1842.21
	SD		772.85	415.09	539.36
Secondary Canal Minimum Diameter	Mean		26.82	23.69	19.19
	SD		9.22	4.25	2.33
Secondary Canal Maximum Diameter	Mean		72.63	80.97	99.47
	SD		21.88	14.74	20.63

Table 2 Histomorphometric variables compared between the age groups[1]

Variable	n	$\mathbf{X^2}$	**df**	**p**
Density				
Pr.On	84	5.34	3	0.000*
OPD	84	54.931	3	0.000*
Size				
Pr.On.Ar	77	0.579	3	0.901
$Pr.On.Dm_{min}$	76	10.628	3	0.014*
$Pr.On.Dm_{max}$	76	12.559	3	0.006*
On.ar	64	8.158	2	0.017*
$On.Dm_{min}$	64	1.430	2	0.489
$On.Dm_{max}$	64	13.890	2	0.001*
H.ar	64	0.393	2	0.822
$H.Dm_{min}$	64	12.096	2	0.002*
$H.Dm_{max}$	64	13.388	2	0.001*

1=Age groups and descriptive statistics are in Table 1

Table 3 Post-hoc tests[1] of the signifiant histomorphometric variables in Table 2

	Statistic	**p**	**Statistic**	**p**
DENSITY	**Pr.On**		**OPD**	
Adolescent v Older child	28.013	0.004*	-16.146	0.050*
Adolescent v Younger child	40.405	0.000*	-44.405	0.000*
Adolescent v Infant	59.452	0.000*	-63.464	0.000*
Older child v Younger child	12.392	0.316	-22.259	0.000*
Older child v Infant	31.439	0.030*	-47.318	0.000*
Young child v Infant	19.048	0.435	19.060	0.427
GEOMETRIC	**$Pr.On.Dm_{min}$**		**$Pr.On.Dm_{max}$**	
Adolescent v Older child	-31.901	0.001*	28.810	0.002*
Adolescent v Younger child	-25.238	0.005*	30.355	0.001*
Adolescent v Infant	-26.310	0.032*	34.595	0.004*
Older child v Younger child	5.952	1.000	1.546	0.792
Older child v Infant	4.881	1.000	5.786	0.566
Young child v Infant	-1.071	1.000	4.240	0.656
	On.Ar		**$On.Dm_{max}$**	
Adolescent v Older child	-10.123	0.117	-11.162	0.080
Adolescent v Younger child	-17.456	0.005*	-22.250	0.002*
Older child v Younger child	-7.332	0.170	-11.088	0.037*
	$H.Dm_{min}$		**$H.Dm_{max}$**	
Adolescent v Older child	17.256	0.006*	-14.234	0.025*
Adolescent v Younger child	20.679	0.001*	-22.286	0.000*
Older child v Younger child	3.153	0.552	-8.052	0.129

1=Dunn-Bonferroni post hoc test. *P value <0.05 significant

Table 4 Linear regression analyses of the relationship between histomorphometric variables and age

Variable[1]	N	Intercept	Slope	R	P	Residual
Pr.On	84	5.34	-0.26	-0.67	0.00*	51%
OPD	84	-1.12	0.59	0.88	0.00*	22%
Pr.On.Ar	77	1172.20	6.08	0.10	0.48	97%
$Pr.On.Dm_{min}$	77	17.56	0.24	0.27	0.03*	92%
$Pr.On.Dm_{max}$	77	69.99	-0.66	-0.19	0.11	96%
On.Ar	64	25973.00	837.02	0.40	0.00*	84%
$On.Dm_{min}$	64	130.91	-0.53	-0.09	0.45	99%
$On.Dm_{max}$	64	215.97	9.78	0.52	0.00*	72%
H.Ar	65	1702.90	8.17	0.08	0.58	96%
$H.Dm_{min}$	65	27.64	-0.48	-0.38	0.02*	81%
$H.Dm_{max}$	65	61.00	2.23	0.45	0.00*	80%

1 = See methods section for definitions. *P value <0.05 significant.